Journal of Biomedical Optics

BiomedicalOptics.SPIEDigitalLibrary.org

Concentration of FAD as a marker for cervical precancer detection

Bharat L. Meena
Asha Agarwal
Chayanika Pantola
Kiran Pandey
Asima Pradhan

SPIE.

Bharat L. Meena, Asha Agarwal, Chayanika Pantola, Kiran Pandey, Asima Pradhan, "Concentration of FAD as a marker for cervical precancer detection," *J. Biomed. Opt.* **24**(3), 035008 (2019), doi: 10.1117/1.JBO.24.3.035008.

Concentration of FAD as a marker for cervical precancer detection

Bharat L. Meena,[a,b] Asha Agarwal,[c] Chayanika Pantola,[d] Kiran Pandey,[e] and Asima Pradhan[a,f,*]
[a]Indian Institute of Technology Kanpur, Department of Physics, Kanpur, Uttar Pradesh, India
[b]University of Rajasthan, Department of Physics, Jaipur, Rajasthan, India
[c]Regency Hospital, Department of Pathology, Kanpur, Uttar Pradesh, India
[d]LPS Institute of Cardiology, Department of Pathology, Kanpur, Uttar Pradesh, India
[e]GSVM Medical College, Department of Obstetrics and Gynaecology, Kanpur, Uttar Pradesh, India
[f]Indian Institute of Technology Kanpur, Center for Lasers and Photonics, Kanpur, Uttar Pradesh, India

Abstract. We report the *ex vivo* results of an in-house fabricated portable device based on polarized fluorescence measurements in the clinical environment. This device measures the polarized fluorescence and elastic scattering spectra with 405-nm laser and white light sources, respectively. The dominating fluorophore with 405-nm excitation is flavin adenine dinucleotide (FAD) with a fluorescence peak around 510 nm. The measured spectra are highly modulated by the interplay of scattering and absorption effects. Due to this, valuable information gets masked. To reduce these effects, intrinsic fluorescence was extracted by normalizing polarized fluorescence spectra with polarized elastic scattering spectra obtained. A number of fluorophores contribute to the fluorescence spectra and need to be decoupled to understand their roles in the progression of cancer. Nelder–Mead method has been utilized to fit the spectral profile with Gaussian to decouple the different bands of contributing fluorophores (FAD and porphyrin). The change in concentration of FAD during disease progression manifests in the change in ratio of total area to FWHM of its Gaussian profile. Receiver operating characteristic (ROC) curve analysis has been used to discriminate different grades of cervical precancer by using the ratio as input parameter. The sensitivity and specificity for discrimination of normal samples from CIN I (cervical intraepithelial neoplasia) are 75% and 54%, respectively. Further, the normal samples can be discriminated from CIN II samples with 100% and 82% sensitivity and specificity, respectively, and the CIN I from CIN II samples can also be discriminated with 100% sensitivity and 90% specificity, respectively. The results show that the change in the concentration of (FAD) can be used as a marker to discriminate the different grades of the cancer and biochemical changes at an early stage of the cancer can also be monitored with this technique. [DOI: 10.1117/1.JBO.24.3.035008]

Keywords: cervical precancer; intrinsic fluorescence; concentration variation; polarized fluorescence.

Paper 180543RR received Sep. 15, 2018; accepted for publication Feb. 22, 2019; published online Mar. 22, 2019.

1 Introduction

Fluorescence spectroscopy is a sensitive technique, applied extensively for detection of different types of cancers. It has the potential to monitor the biochemical changes that take place during the disease progression.[1–4] The spectroscopic study of breast tissue was pioneered by Alfano et al.,[5] and Feld et al.[6] applied it to human aorta tissue. Subsequently different research groups worked on its application for detection of breast cancer.[7–10] Autofluorescence from buccal mucosa has been used by Schwarz et al.,[11] Madhuri et al.,[12] and Kumar et al.[13] in oral cancer detection. Several groups have worked on diagnosis of cervical precancer using laser-induced fluorescence spectroscopy[14,15] and in combination with reflectance spectroscopy[16–18] for comparison and to improve the detection efficacy. Intrinsic fluorescence[19–21] has also been extracted to understand the biochemical changes with disease progression through different experimental[22] and simulation-based techniques.[23–26] The use of different algorithms, such as machine learning,[27] wavelet analysis,[9] and other multivariate algorithms[10,20,28,29] have made detection more effective and robust.

As mentioned above, the natural fluorescences are taken as markers for detection of disease. It is well known that biological tissue has several natural fluorophores with absorption and fluorescence spectra in UV–VIS range.[12,30–33] The development of the cancer is associated with the changes taking place in tissue optical properties, which includes changes in the concentration of contributing fluorophores, such as flavin adenine dinucleotide (FAD), reduced form of nicotinamide adenine dinucleotide (NADH), and change in collagen cross-links in stroma.[31,32] Further, the morphological and microvascularization changes results in variation in scattering and absorption properties of the biological tissue sample.[8,24,29] The fluorescence features in biological tissue can be distorted significantly due to scattering and absorption effects. Hence extraction of intrinsic fluorescence is needed to monitor the relative changes in the concentration of contributing fluorophores.[20,22–26,34] Earlier, Biswal et al.[22] developed an experimental technique to extract the intrinsic fluorescence based on polarized fluorescence and polarized scattering measurements, which is free from absorption and scattering effects. Further *ex vivo* studies on biopsy samples of the cervix have illustrated the efficacy of this technique.[19,20] This has led to the fabrication of a portable device for *in vivo* detection of cervical precancer.[20]

In this study, we report the *ex vivo* results from the portable device, by using the change in the concentration of FAD as a marker for early cervical cancer detection. A number of

*Address all correspondence to Asima Pradhan, E-mail: asima@iitk.ac.in

fluorophores contribute to the broad fluorescence spectrum when tissue is excited at 405 nm. These fluorophores need to be decoupled to understand their roles in the progression of cancer.[35] Nelder–Mead method has been utilized to fit the spectral profile with Gaussian to decouple the different bands of contributing fluorophores (FAD and porphyrin).[20,31] The change in concentration of FAD during disease progression manifests in the change in ratio of total area and FWHM of its Gaussian profile. Receiver operating characteristic (ROC) curve analysis has been used to discriminate different grades of cervical precancer by using the ratio as input parameter.

2 Materials and Methods

2.1 *Instrumentation*

Figure 1 shows the schematic of the experimental setup used for the measurements of polarized fluorescence and polarized elastic scattering spectra from total hysterectomy samples. The details of the system have been discussed in other references.[20,21] In brief, two light sources, a 405-nm diode laser (Pegasus, Shanghai, Optical System Co. Ltd.) and a white light source (Xe-lamp, Newport Oriel Instruments) were used for polarized fluorescence and polarized elastic scattering measurements, respectively. A miniature spectrometer (HR2000+, Ocean Optics, Inc., Dunedin, Florida) was used for collection of spectra. The sample was illuminated with focused vertically polarized light through different optical components. Fluorescence and scattering signals were collected sequentially from the same site of the sample with different integration times in co- and crosspolarization states in backscattering mode and background corrections were done separately for each.

2.2 *Sample Handling and Analysis Method*

The study protocol was approved by institutional ethics committee at IIT Kanpur, India, and GSVM Medical College Kanpur, India, under the protocol number IITK/IEC/2012-13/1/3. The study was performed in the hospital (at GSVM Medical College) on the total hysterectomy samples. Figure 2 shows the schematic representation of the study protocol followed during the study on the hysterectomy cervical samples in the clinical environment. The details of sample handling and data acquisition have been discussed elsewhere.[20] The doctors involved in this study ensured that a written consent was obtained from each patient before the experiment was performed. A total of 156 sites of 28 patients include, 68 normal sites of 13 patients, 72 CIN I sites of 13 patients, and 16 sites of 2 patients from different social backgrounds and age groups were tested, and they were divided into different groups according to postbiopsy findings. A long time delay after the operation degrades the contribution from different fluorophores, mainly the contribution

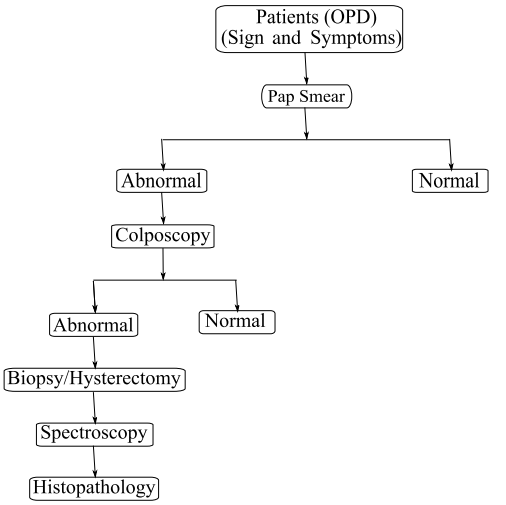

Fig. 2 Schematic representation of the *ex vivo* study protocol in the clinical environment with the cervical hysterectomy tissue samples.

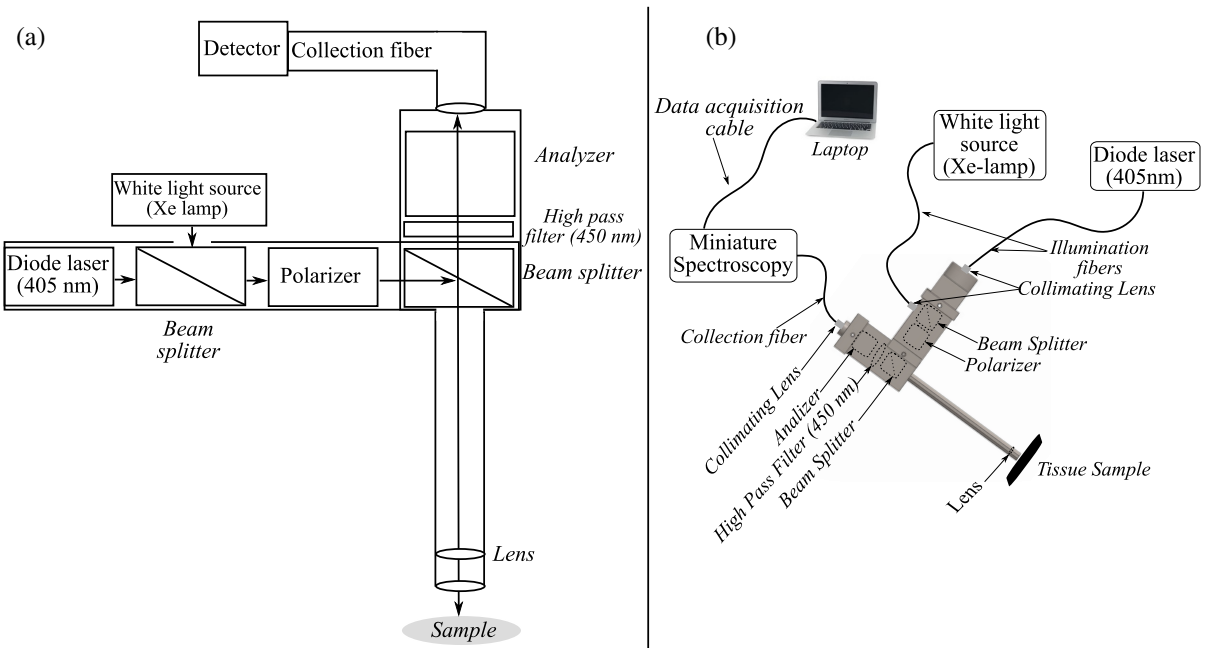

Fig. 1 (a) Schematic block diagram and (b) cartoon representation of the experimental setup for polarized fluorescence measurements from cervical hysterectomy tissue samples.

of the porphyrin.[21] Therefore, the measurements on the total hysterectomy samples has been perform immediately after the operation in the hospital within time delay of 5 to 10 min, which minimized the loss of the signal. Intrinsic fluorescence was extracted from the measured data using[19–22]

$$\mathrm{IF} = \frac{[I_{\mathrm{vv}}(\lambda) - G(\lambda) * I_{\mathrm{vh}}(\lambda)]_{\mathrm{fl}}}{[I_{\mathrm{vv}}(\lambda) - G(\lambda) * I_{\mathrm{vh}}(\lambda)]_{\mathrm{scat}}}, \quad (1)$$

where $I_{vv}(\lambda)$ and $I_{\mathrm{vh}}(\lambda)$ are the co- and crosspolarized signals, respectively. Subscript "fl" and "scat" represent the fluorescence and scattering, respectively. $G(\lambda) = I_{\mathrm{hh}}(\lambda)/I_{\mathrm{hv}}(\lambda)$ is the ratio of the sensitivity of the instrument to the vertically and horizontally polarized light, keeping the source light in horizontal polarized state.

After extraction of intrinsic fluorescence, Nelder–Mead method has been utilized to fit the spectral profile with Gaussian to decouple the different bands of contributing fluorophores (FAD and porphyrin). The change in concentration of FAD during disease progression manifests in the change in ratio of total area and FWHM of its Gaussian profile. ROC curve analysis has been used to discriminate different grades of cervical precancer samples from normal cervical samples by using the ratio as input parameter.

3 Results and Discussion

Figures 3(a) and 3(b) show the co- and crosspolarized fluorescence spectra, respectively, from normal and CIN I counterpart of the same sample. The major fluorescence bands of FAD (peak at 510 nm) and porphyrin (peaks at 590 and 650 nm) have been observed.[20,31] The elimination of absorption and scattering effects in extracted intrinsic fluorescence spectra of normal and CIN I can be seen in Fig. 3(c). The fluorescence intensity from the normal site of the sample is found to be higher than that with CIN I site of the same sample, as expected, due to the conversion of FAD to its reduced form with disease progression.[12,33] Figure 3(d) shows the area normalized polarized fluorescence, polarized elastic scattering, and extracted intrinsic fluorescence spectra of CIN I sample. The absorption dips of hemoglobin/oxyhemoglobin are evident in polarized fluorescence and polarized elastic scattering spectra at 476, 527, and 556 nm.[20]

Figures 4(a) and 4(b) show the typical fitted curves with Nelder–Mead method and the bottom plots show the residual spectra obtained from the corresponding Gaussian fit of the area normalized signals of normal, and CIN I counterparts of the same sample, respectively. The fitting was done by fixing the position of the different peaks and the total area under the different contributing fluorescence peaks and FWHM were calculated. A similar process was followed for co-polarized and crosspolarized spectra (not shown here). The ratio of the area under the FAD peak to the FWHM was used as input in ROC analysis. Figures 5(a) and 5(b) show the scatter plots of the ratio, using intrinsic fluorescence for the discrimination of CIN I and CIN II samples from normal, respectively, and the discrimination of CIN I from CIN II samples is shown in Fig. 5(c). Figure 5(d) shows the ROC analysis with the ratio from extracted intrinsic fluorescence signal of different grades of the cervical samples. The sensitivity and specificity for the discrimination of normal from CIN I samples is low but the discrimination of higher grade from normal and from CIN I is high (shown in 1). Figures 6(a)–6(c) show the scatter plot of the ratio for copolarized fluorescence spectra and the ROC analysis for normal versus CIN I, normal versus CIN II, and CIN I versus CIN II are shown in Fig. 6(d). Similarly, the analysis was done with cross-polarized fluorescence signal also and shown in Figs. 7(a)–7(d).

The statistical findings of the analysis are shown in Table 1. As is evident from the table, normal and CIN I are well discriminated from CIN II with high sensitivity and specificity. The results show that although the sensitivity of discrimination of

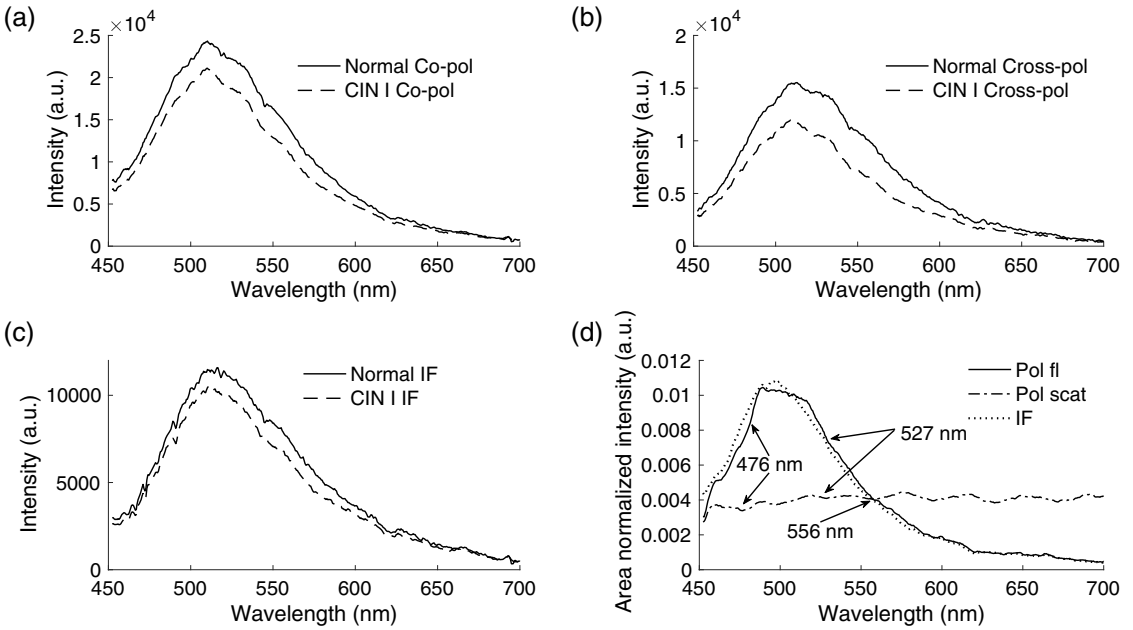

Fig. 3 Typical fluorescence spectra of normal and CIN I counterparts of the same sample: (a) copolarized fluorescence, (b) crosspolarized fluorescence, (c) intrinsic fluorescence, and (d) area normalized polarized fluorescence, polarized elastic scattering, and intrinsic fluorescence spectra of CIN I counter part of the sample.

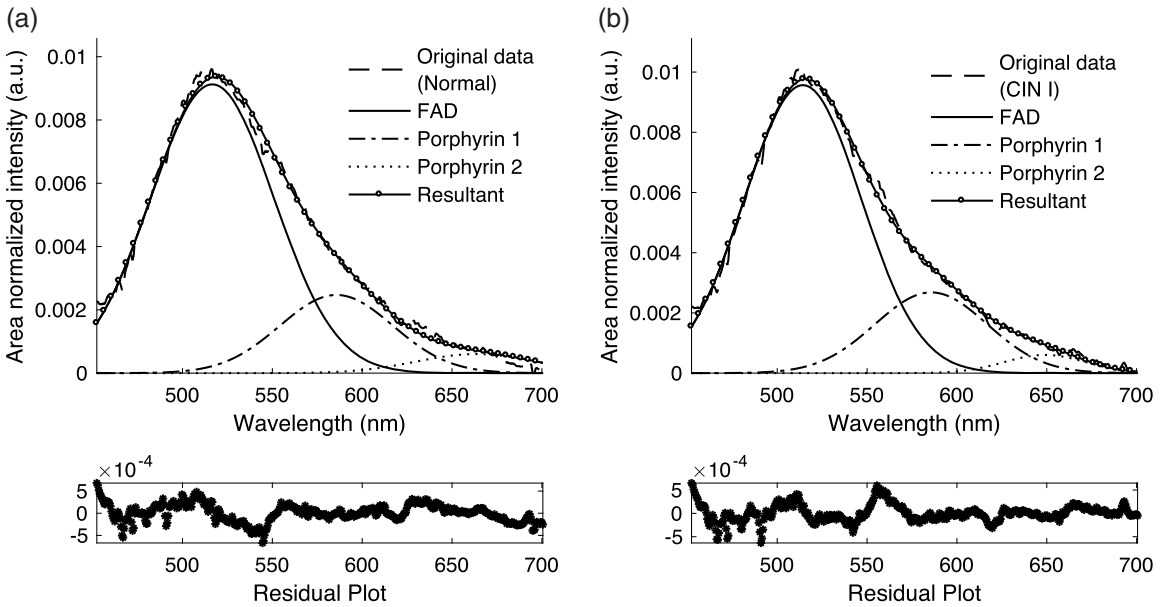

Fig. 4 Typical fitted intrinsic fluorescence spectra of (a) normal and (b) CIN I counterparts of the same sample (bottom plot shows the residual of the corresponding plot).

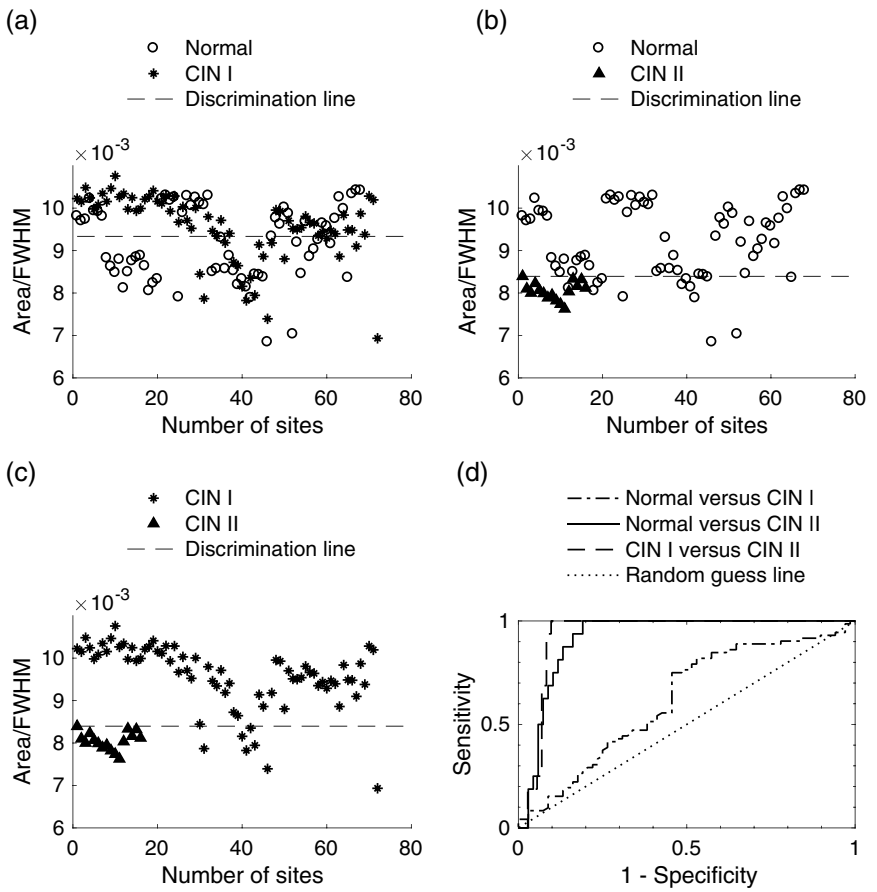

Fig. 5 Scatter plot of the ratio of the area under the curve and the FWHM of the fitted curve for FAD peak to discriminate different class pairs using intrinsic fluorescence: (a) normal versus CIN I, (b) normal versus CIN II, (c) CIN I versus CIN II, and (d) ROC curves sowing the discrimination efficiency of the ratio for different class pairs.

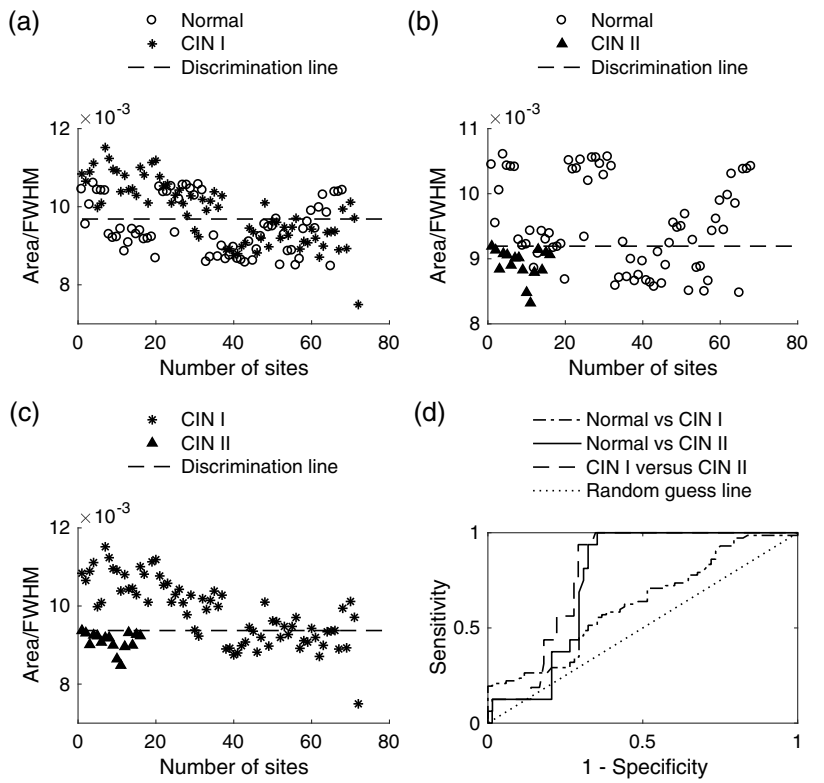

Fig. 6 Scatter plot of the ratio of the area under the curve and the FWHM of the fitted curve for FAD peak to discriminate different class pairs using copolarized fluorescence: (a) normal versus CIN I, (b) normal versus CIN II, (c) CIN I versus CIN II, and (d) ROC curves sowing the discrimination efficiency of the ratio for different class pairs.

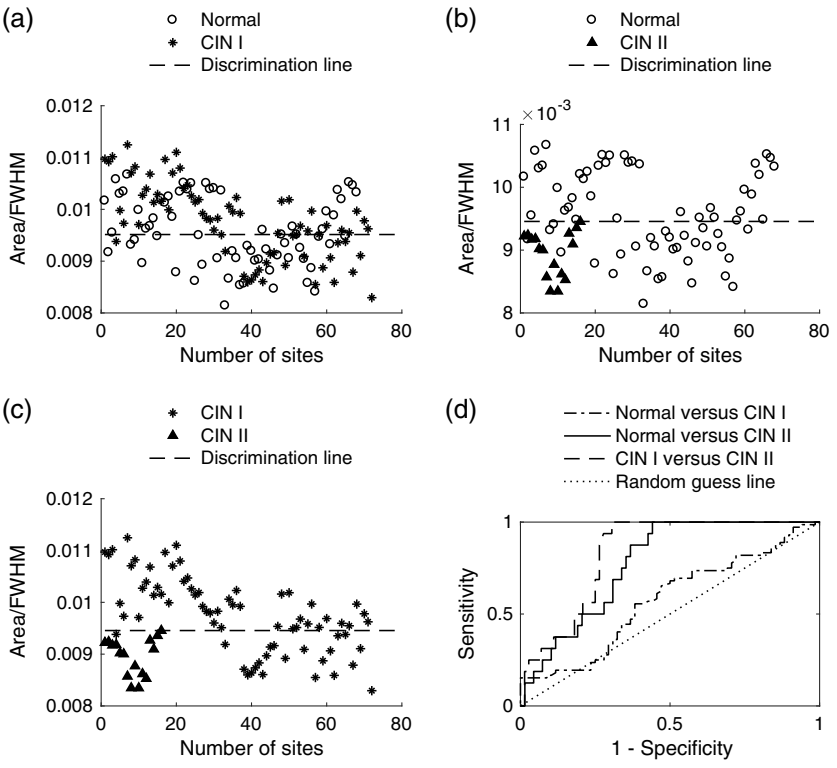

Fig. 7 Scatter plot of the ratio of the area under the curve and the FWHM of the fitted curve for FAD peak to discriminate different class pairs using cross-polarized fluorescence: (a) normal versus CIN I, (b) normal versus CIN II, (c) CIN I versus CIN II, and (d) ROC curves sowing the discrimination efficiency of the ratio for different class pairs.

Table 1 Statistical findings of the classification of different tissue classes of the cervical hysterectomy samples with intrinsic fluorescence, copolarized fluorescence, and crosspolarized fluorescence spectra.

Tissue classes	Sensitivity (%)	Specificity (%)
Intrinsic fluorescence		
Normal versus CIN I	75	54
Normal versus CIN II	100	82
CIN I versus CIN II	100	90
Copolarized fluorescence		
Normal versus CIN I	55	64
Normal versus CIN II	100	64
CIN I versus CIN II	100	65
Crosspolarized fluorescence		
Normal versus CIN I	65	52
Normal versus CIN II	100	55
CIN I versus CIN II	100	69

normal and CIN I from CIN II with co- and crosspolarized spectra is similar to intrinsic fluorescence, the specificity in both cases is low as compare to intrinsic fluorescence. The advantage of reducing absorption and scattering effects in the extracted intrinsic fluorescence is thus evident. The results show that the change in the concentration of FAD can be used as a marker to discriminate the different grades of the cancer, and biochemical changes at early stage of the cancer can also be monitored using intrinsic fluorescence.

Disclosures

The authors have no relevant financial interests in this article and no potential conflicts of interest to disclose.

Acknowledgments

Asima Pradhan wishes to acknowledge the IMPRINT, MHRD, Govt. of India (Grant No. CELP/MHRD/2016408K) and Society for Research and Initiatives for Sustainable Technologies and Institutions (SRISTI), Ahmedabad, Gujarat, India (Grant No. BIRAC/PHY/2016353) for funding the research. Bharat Lal Meena acknowledges Society for Research and Initiatives for Sustainable Technologies and Institutions (SRISTI), Ahmedabad, Gujarat, India for funding the research (Grant No. BIRAC/PHY/2016353).

References

1. T. Novikova, "Optical techniques for cervical neoplasia detection," *Beilstein J. Nanotechnol.* **8**, 1844–1862 (2017).
2. B. Yu et al., "Emerging optical techniques for detection of oral, cervical and anal cancer in low-resource settings," *Austin J. Biomed. Eng.* **1**(2), 1007 (2014).
3. M. Olivo, C. J. H. Ho, and C. Y. Fu, "Advances in fluorescence diagnosis to track footprints of cancer progression in vivo," *Laser Photonics Rev.* **7**(5), 646–662 (2013).
4. K. Sokolov, M. Follen, and R. Richards-Kortum, "Optical spectroscopy for detection of neoplasia," *Curr. Opin. Chem. Biol.* **6**(5), 651–658 (2002).
5. R. Alfano et al., "Fluorescence spectra from cancerous and normal human breast and lung tissues," *IEEE J. Quantum Electron.* **23**(10), 1806–1811 (1987).
6. M. Keijzer et al., "Fluorescence spectroscopy of turbid media: autofluorescence of the human aorta," *Appl. Opt.* **28**(20), 4286–4292 (1989).
7. G. Tang et al., "Pulsed and CW laser fluorescence spectra from cancerous, normal, and chemically treated normal human breast and lung tissues," *Appl. Opt.* **28**(12), 2337–2342 (1989).
8. M. S. Nair et al., "Determination of optical parameters of human breast tissue from spatially resolved fluorescence: a diffusion theory model," *Appl. Opt.* **41**(19), 4024–4035 (2002).
9. N. Agarwal et al., "Wavelet transform of breast tissue fluorescence spectra: a technique for diagnosis of tumors," *IEEE J. Sel. Top. Quantum Electron.* **9**(2), 154–161 (2003).
10. A. H. Gharekhan et al., "Characterizing breast cancer tissues through the spectral correlation properties of polarized fluorescence," *J. Biomed. Opt.* **13**(5), 054063 (2008).
11. R. A. Schwarz et al., "Noninvasive evaluation of oral lesions using depth-sensitive optical spectroscopy," *Cancer* **115**(8), 1669–1679 (2009).
12. S. Madhuri et al., "Native fluorescence spectroscopy of blood plasma in the characterization of oral malignancy," *Photochem. Photobiol.* **78**(2), 197–204 (2003).
13. P. Kumar et al., "Human saliva for oral precancer detection: a comparison of fluorescence & stokes shift spectroscopy," *J. Fluoresc.* **28**(1), 419–426 (2018).
14. N. Ramanujam et al., "Spectroscopic diagnosis of cervical intraepithelial neoplasia (cin) in vivo using laser-induced fluorescence spectra at multiple excitation wavelengths," *Lasers Surg. Med.* **19**(1), 63–74 (1996).
15. R. Richards-Kortum et al., "In vivo fluorescence spectroscopy: potential for non-invasive, automated diagnosis of cervical intraepithelial neoplasia and use as a surrogate endpoint biomarker," *J. Cell. Biochem.* **19**(Suppl.), 111–119 (1994).
16. J. A. Freeberg et al., "The clinical effectiveness of fluorescence and reflectance spectroscopy for the in vivo diagnosis of cervical neoplasia: an analysis by phase of trial design," *Gynecol. Oncol.* **107**(1), S270–S280 (2007).
17. K. T. Schomacker et al., "Novel optical detection system for in vivo identification and localization of cervical intraepithelial neoplasia," *J. Biomed. Opt.* **11**(3), 034009 (2006).
18. R. J. Nordstrom et al., "Identification of cervical intraepithelial neoplasia (cin) using uv-excited fluorescence and diffuse-reflectance tissue spectroscopy," *Lasers Surg. Med.* **29**(2), 118–127 (2001).
19. S. Devi, P. K. Panigrahi, and A. Pradhan, "Detecting cervical cancer progression through extracted intrinsic fluorescence and principal component analysis," *J. Biomed. Opt.* **19**(12), 127003 (2014).
20. B. L. Meena et al., "Intrinsic fluorescence for cervical precancer detection using polarized light based in-house fabricated portable device," *J. Biomed. Opt.* **23**(1), 015005 (2018).
21. B. L. Meena et al., "Intrinsic fluorescence based in-vivo detection of cervical precancer with hand held prototype device," *Proc. SPIE* **10489**, 104891G (2018).
22. N. C. Biswal et al., "Recovery of turbidity free fluorescence from measured fluorescence: an experimental approach," *Opt. Express* **11**(24), 3320–3331 (2003).
23. J. Wu, M. S. Feld, and R. P. Rava, "Analytical model for extracting intrinsic fluorescence in turbid media," *Appl. Opt.* **32**(19), 3585–3595 (1993).
24. S. Gupta, V. S. Raja, and A. Pradhan, "Simultaneous extraction of optical transport parameters and intrinsic fluorescence of tissue mimicking model media using a spatially resolved fluorescence technique," *Appl. Opt.* **45**(28), 7529–7537 (2006).
25. G. M. Palmer and N. Ramanujam, "Monte-Carlo-based model for the extraction of intrinsic fluorescence from turbid media," *J. Biomed. Opt.* **13**(2), 024017 (2008).
26. M. G. Müller et al., "Intrinsic fluorescence spectroscopy in turbid media: disentangling effects of scattering and absorption," *Appl. Opt.* **40**(25), 4633–4646 (2001).

27. J. Xue et al., "Machine learning based analysis of human prostate cancer cell lines at different metastatic ability using native fluorescence spectroscopy with selective excitation wavelength," *Proc. SPIE* **10504**, 105040L (2018).
28. H. Zhu et al., "Multivariate functional response regression, with application to fluorescence spectroscopy in a cervical pre-cancer study," *Comput. Stat. Data Anal.* **111**, 88–101 (2017).
29. R. J. Mallia et al., "Clinical grading of oral mucosa by curve-fitting of corrected autofluorescence using diffuse reflectance spectra," *Head Neck* **32**(6), 763–779 (2010).
30. J. Lakowicz, *Principles of Fluorescence Spectroscopy*, Springer, New York (2007).
31. R. Alfano and Y. Yang, "Stokes shift emission spectroscopy of human tissue and key biomolecules," *IEEE J. Sel. Top. Quantum Electron.* **9**(2), 148–153 (2003).
32. R. Drezek et al., "Understanding the contributions of NADH and collagen to cervical tissue fluorescence spectra: modeling, measurements, and implications," *J. Biomed. Opt.* **6**(4), 385–396 (2001).
33. R. Alfano et al., "Laser induced fluorescence spectroscopy from native cancerous and normal tissue," *IEEE J. Quantum Electron.* **20**(12), 1507–1511 (1984).
34. R. S. Bradley and M. S. Thorniley, "A review of attenuation correction techniques for tissue fluorescence," *J. R. Soc. Interface* **3**(6), 1–13 (2006).
35. A. Pradhan et al., "Fluorescence study of normal, benign, and malignant human breast tissues," *Proc. SPIE* **3917**, 240–243 (2000).

Bharat L. Meena is a research scholar at Indian Institute of Technology Kanpur and an assistant professor at the University of Rajasthan Jaipur. He received his MS degree in physics from the University of Delhi in 2010. His research interests have been in the area of biophotonics. The recent focus lies in the development of a portable device for detection of cervical cancer at an early stage, using polarized light.

Kiran Pandey is one of the senior most gynecologists of India, who heads the Department of OBG at GSVM Medical College, Kanpur. Her areas of expertise include gyne oncology, infertility, urogynecology, and high risk pregnancy. She is the secretary of the U.P chapter of Association of Gyne Oncologists of India. She has published more than 100 research papers in national and international journals. She has been bestowed with 11 national level, 8 state level, and numerous district level awards.

Asima Pradhan is a professor in the Department of Physics at the Indian Institute of Technology (IIT), Kanpur, India, and is also associated with the Center for Lasers and Photonics. She received her PhD from City University of New York in 1991. Her areas of interest include laser spectroscopy and biophotonics. Her expertise is in fluorescence spectroscopy, light scattering spectroscopy, time-resolved fluorescence, polarization-based fluorescence, and Mueller matrix imaging of biosamples.

Biographies of the other authors are not available.